

# *Study of Streptavidin-Modified Quantum Dots by Capillary Electrophoresis*

**Maja Stanisavljevic, Libor Janu, Kristyna Smerkova, Sona Krizkova, Nadezda Pizurova, Marketa Ryvolova, Vojtech Adam, Jaromir Hubalek, et al.**

## **Chromatographia**

An International Journal for Rapid Communication in Chromatography, Electrophoresis and Associated Techniques

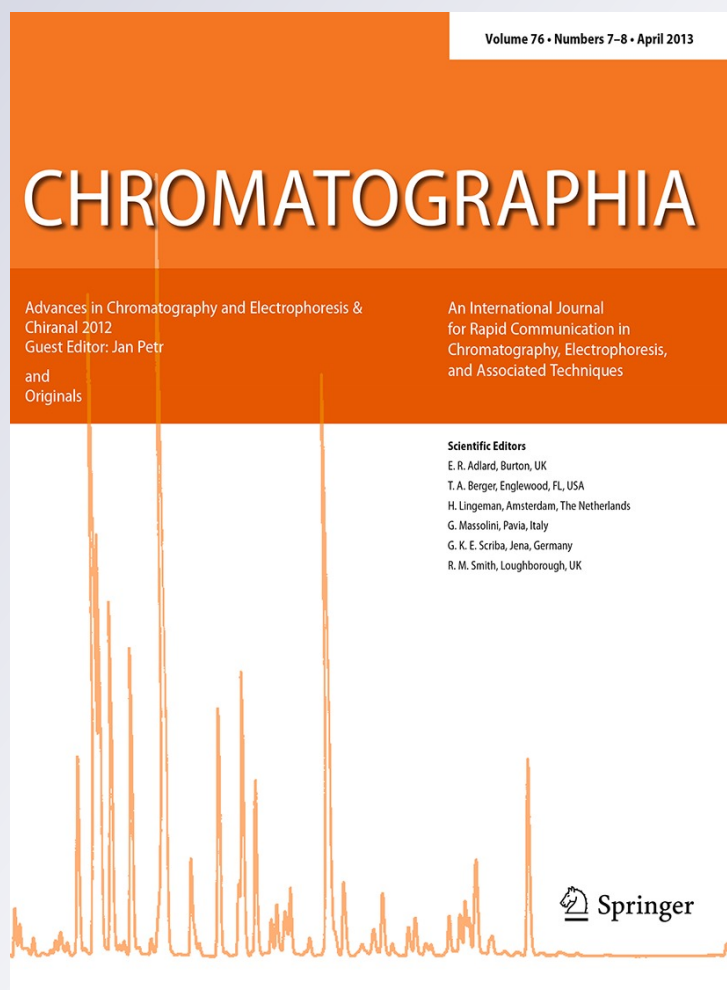
ISSN 0009-5893

Volume 76

Combined 7-8

Chromatographia (2013) 76:335-343

DOI 10.1007/s10337-012-2372-8



**Your article is protected by copyright and all rights are held exclusively by Springer-Verlag Berlin Heidelberg. This e-offprint is for personal use only and shall not be self-archived in electronic repositories. If you wish to self-archive your work, please use the accepted author's version for posting to your own website or your institution's repository. You may further deposit the accepted author's version on a funder's repository at a funder's request, provided it is not made publicly available until 12 months after publication.**

# Study of Streptavidin-Modified Quantum Dots by Capillary Electrophoresis

Maja Stanisavljevic · Libor Janu · Kristyna Smerkova ·  
Sona Krizkova · Nadezda Pizurova · Marketa Ryvolova ·  
Vojtech Adam · Jaromir Hubalek · Rene Kizek

Received: 28 June 2012/Revised: 31 October 2012/Accepted: 30 November 2012/Published online: 25 December 2012  
© Springer-Verlag Berlin Heidelberg 2012

**Abstract** Great boom of nanotechnologies impacts almost all areas of science and therefore detail understanding of the properties of nanomaterials as well as their interaction abilities is required. Surface modification and functionalization of nanoparticles is of a great interest due to the wide range of applications in the area of nanomedicine, nanobiology, and/or biochemistry. In this study, CdTe QDs were synthesized using microwave reactor and their surface was modified by streptavidin to ensure further suitability for bioconjugation with biotin-labelled oligonucleotides. For characterization of the synthesized QDs and for monitoring of the interaction with the oligonucleotide, capillary and gel electrophoresis was used. Moreover, complementary advantages of absorption (CE–UV) and laser-induced fluorescence detection (CE–LIF) were exploited. Comparison the electrophoretic mobilities obtained for streptavidin-modified QDs by CE–LIF ( $-9.87 \times 10^{-9} \text{ m}^2/\text{V/s}$ ) and by CE–UV ( $-10.02 \times$

$10^{-9} \text{ m}^2/\text{V/s}$ ) was in a good agreement enabling us to identify the peak of streptavidin-modified QDs in the CE–UV electropherogram containing also the peak of unreacted streptavidin. Subsequent conjugation of streptavidin-modified QDs with two model biotinylated oligonucleotides (BCL-2 and HBV) led to formation of the complex represented in the electropherograms as a very sharp peak. This peak height increased with time for 15.5 and 27 mAU using BCL-2 oligonucleotide and HBV oligonucleotide, respectively during 30 min interaction.

**Keywords** Capillary electrophoresis · Gel electrophoresis · Avidin–biotin technology · Oligonucleotide · Nanoparticle, quantum dots

## Introduction

Streptavidin–biotin is one of the most commonly used bioconjugation approach due to the high affinity between biotin and streptavidin [1–3]. Therefore, it is not surprising that this technology is being also utilized in nanotechnology as one of the rapidly growing field of scientific interest [4, 5]. Nanotechnology is a multidisciplinary scientific field, which involves creation and utilization of nanoscale materials [6–10]. Quantum dots (QDs) are nanomaterials made of semiconductors, which have size-depending electronic and optical properties, which are between atoms and bulk materials [11, 12]. Due to convincing optical properties, QDs are new fluorescent materials, which are used instead of organic dyes for biological labelling. They have better photostability than organic dyes, narrow emission and continuous absorption spectra [13]. QDs applications are widespread such as for early detection of cancer, for drug delivery, in vivo imaging and targeting [9, 10, 14–18].

Published in the special paper collection *Advances in Chromatography and Electrophoresis & Chiral 2012* with guest editor Jan Petr.

M. Stanisavljevic · L. Janu · K. Smerkova · S. Krizkova ·  
M. Ryvolova · V. Adam · J. Hubalek · R. Kizek (✉)  
Department of Chemistry and Biochemistry,  
Faculty of Agronomy, Mendel University in Brno,  
Zemedelska 1, 613 00 Brno, Czech Republic  
e-mail: kizek@sci.muni.cz

S. Krizkova · M. Ryvolova · V. Adam · J. Hubalek · R. Kizek  
Central European Institute of Technology,  
Brno University of Technology, Technicka 3058/10,  
616 00 Brno, Czech Republic

N. Pizurova  
Institute of Physics of Materials, Academy of Sciences  
of the Czech Republic, Zizkova 22, 616 62 Brno,  
Czech Republic

Due to the toxicity of their inorganic core, the surface of QDs has to be chemically modified. Thiol-group containing compounds such as mercaptopropionic acid [19], glutathione [20] and/or cysteine [21] are commonly used as capping agents. After modification, QDs are suitable for conjugation with biomolecules such as proteins, fragments of DNA and/or RNA, however, some covalent and non-covalent attachment methodologies must be applied. Common covalent conjugation is based on streptavidin–biotin linkage and non-covalent linkage is achieved through simple electrostatic linkage [22]. Such conjugated QDs with biomolecules have been successfully applied in biological and medical fields like immunoassay [23], DNA hybridization [24] and/or cell imaging [25].

To characterize nanoparticles, transmission electron microscopy (which is time consuming and very expensive) [26], size exclusion chromatography (very high surface activity may cause problem during measurement) [27], and dynamic light scattering (which is an expensive technique) [28] are usually used. Due to disadvantages, it is necessary to find a fast, effective and easy-to-use method for QDs size measurement and their separation according to size because of their rapidly increasing applications [29]. Capillary electrophoresis (CE) is a powerful separation technique for characterizing nanoparticles in size, shape or charge due to its simplicity, short analysis time, small sample and reagent requirements, high separation efficiency, and extremely high sensitivity. It has already been used to separate a numerous nanomaterials such as inorganic oxide [30], SiO<sub>2</sub> [31], gold and silver nanoparticles [32, 33] and carbon nanotubes [34]. In this study, capillary electrophoresis and gel electrophoresis are used as effective methods for quality control, functionality verification and interaction monitoring of streptavidin-modified CdTe QDs synthesized by rapid and efficient method using microwave reactor.

## Experimental

### Chemicals

All chemicals were purchased from Sigma Aldrich (St. Louis, MA, USA) in ACS purity. Solutions were made using MiliQ water (Milipore, Prague, Czech Republic). Oligonucleotide sequences were as follows: cancer sequence BCL-2: BIOTIN -5'-TCT CCC GGC TTG CGC CAT-3' [35], viral VHB: BIOTIN-5' CAT CCT GCT GCT ATG CCT CAT CT 3' [36].

### QDs Synthesis

CdTe QDs were prepared by microwave synthesis (Anton Paar, Wien, Austria) and capped by mercaptopropionic acid

(MPA) according to the following procedure: the solution of CdCl<sub>2</sub> (4 mL, 0.04 M) was mixed with Na<sub>2</sub>TeO<sub>3</sub> (4 mL, 0.01 M), 100 mg of sodium citrate and 50 mg NaBH<sub>4</sub>, 119 mg MPA and 42 mL of H<sub>2</sub>O. The mixture was heated by microwave radiation for 10 min (300 W). The product was precipitated by isopropanol to remove the excessive reagents according to the following: 1 mL of CdTe QDs solution was mixed with 1 mL of isopropanol and centrifuged. The supernatant was removed and precipitated CdTe QDs were dissolved in 1 mL of ACS water [37].

### TEM Characterization

Morphology studies were carried out with the transmission electron microscope (TEM) Philips CM 12 (tungsten cathode, using a 120 kV electron beam). Samples for TEM measurements were prepared by placing drops of the solution (sample and water) on coated Cu grids (holey carbon and holey SiO<sub>2</sub>/SiO) and subsequently drying in air.

### Streptavidin Modification

100 µL of MPA capped CdTe QDs (MPA-QDs) were diluted to 1 mL and the pH was adjusted to 7 by MPA solution. Streptavidin (9.6 µL, 5 mg/mL) was added and the solution was intensively agitated for 60 min. Subsequently, the solution was centrifuged for 80 min. The supernatant was disposed and the precipitated CdTe QDs-MPA-strep were dissolved in 100 µL of water [38].

### Spectroscopic Analysis

Fluorescence and absorbance spectra were acquired by multifunctional microplate reader Tecan Infinite 200 PRO (TECAN, Männedorf, Switzerland). 350 nm was used as an excitation wavelength and the fluorescence scan was measured within the range from 400 to 850 nm per 5 nm steps. Each intensity value is an average of 5 measurements. The detector gain was set to 100. The absorbance was acquired within the range from 230 to 1,000 nm with 5 nm steps as an average of 5 measurements per well. The sample (50 µL) was placed in transparent 96-well microplate with flat bottom by Nunc (ThermoScientific, Waltham, MA, USA).

### Electrophoretic Analysis

#### *DNA Electrophoresis*

Non-denaturing electrophoresis of DNA was performed in 15 % polyacrylamide gels in TAE buffer (40 mM Tris, 20 mM acetic acid, 1 mM EDTA, pH = 8.0, Bio-Rad, USA) in a Mini Protean Tetra apparatus (Bio-Rad, Hercules, CA, USA) at 120 V for 45 min. After the

electrophoresis was completed, the gels were photographed in In vivo imaging system Xtreme (Carestream Health, Rochester, NY, USA) at excitation wavelength of 510 nm and emission wavelength of 600 nm to visualize the QDs. In order to visualize the ssDNA and dsDNA, the gels were stained with GelRed™ Nucleic Acid Gel Stain (Biotium, Hayward, CA, USA) in dilution 1:5000 in water for 30 min and consequently photographed on a transilluminator at 324 nm. To visualize the proteins, the gels were stained with Coomassie blue according to Wong et al. [39].

#### Sodium Dodecyl Sulphate Polyacrylamide Gel Electrophoresis (SDS-PAGE)

The electrophoresis was performed using a Mini Protean Tetra apparatus with gel dimension of  $8.3 \times 7.3$  cm (Bio-Rad, USA). First 10 % (m/V) running, and then 5 % (m/V) stacking gels were poured. The gels were prepared from 30 % (m/V) acrylamide stock solution with 1 % (m/V) bisacrylamide. The polymerization of the running or stacking gels was carried out at room temperature for 45 min or 30 min, respectively. Prior to analysis the samples were mixed either with reducing (5 %  $\beta$ -mercaptoethanol) or non-reducing sample buffer (50 mM Tris/HCl, 2 % SDS, 20 % glycerol, 0.1 % bromophenol blue, pH = 8.8) in a 1:1 ratio. The samples were incubated at 93 °C for 3 min, and the sample was loaded onto a gel. For determination of the molecular mass, the protein ladder “Precision plus protein standards” from Biorad was used. The electrophoresis was run at 150 V for 1 h at laboratory temperature (23 °C) (Power Basic, Biorad, Hercules, CA, USA) in tris–glycine buffer (0.025 M Trizma-base, 0.19 M glycine and 3.5 mM SDS, pH = 8.3). After the electrophoresis was completed, the gels were photographed in In vivo imaging system Xtreme (Carestream Health, Rochester, NY USA) at excitation wavelength of 470 nm and emission of 535 nm to visualize the QDs. Then, the gels were stained with silver according to Krizkova et al. [40] to visualize proteins.

#### Capillary Electrophoresis

Capillary electrophoresis with UV absorbance detection (CE–UV) measurement was performed using capillary electrophoresis system (Beckman P/ACE 5500, Brea, CA,

USA) at 214 nm and with laser-induced fluorescence detection (CE–LIF) at  $\lambda_{\text{ex}} = 488$  and  $\lambda_{\text{em}} = 520$  nm. An uncoated fused silica capillary with total capillary length of 47 cm, effective length of 40 cm and internal diameter of 75  $\mu\text{m}$  was used. 0.02 M sodium borate (pH 9.2) was used as background electrolyte. Separation was carried out at 20 kV and the sample was injected hydrodynamically for 20 s using 3.4 kPa. Coumarin 334 and coumarin were used as electroosmotic flow (EOF) markers for CE–LIF and CE–UV, respectively.

## Results and Discussion

### Synthesis of CdTe QDs

MPA-capped CdTe QDs were synthesized by rapid microwave synthesis enabling formation of required QDs within 10 min. QDs as modern fluorescent labels require being surface modified to provide both biocompatibility as well as functionality. One of the most important biochemical interactions, biotin–avidin (streptavidin) interaction, plays a key role in QDs functionalization process. Both biotin-modified and streptavidin-modified QDs were utilized for these purposes [41]. In this study, the bioconjugation of CdTe QDs capped with MPA via electrostatic interaction with streptavidin was done. The scheme of formation of bioconjugate QD–streptavidin and biotin-modified oligonucleotide is shown in Fig. 1. Primarily, the metal CdTe nanocrystal is formed and capped by MPA to form a stable and optically active colloidal solution. After isopropanol precipitation the surface was modified by streptavidin to provide required functionality.

Prepared MPA capped CdTe QDs were characterized by TEM and by fluorescent spectroscopy. The characterization of both properties is needed due to their further applications as fluorescent nanoparticles. TEM analysis can reveal dimensions of the particles as well as to confirm the elemental composition. TEM micrograph of CdTe QDs is shown in Fig. 2a. The TEM examination of the QDs sample indicates the morphology and phase composition were clearly homogeneous. The TEM pictures (at higher magnifications) show that dried droplets consisted of a fine grain powder of a typical size of particles below 10 nm.

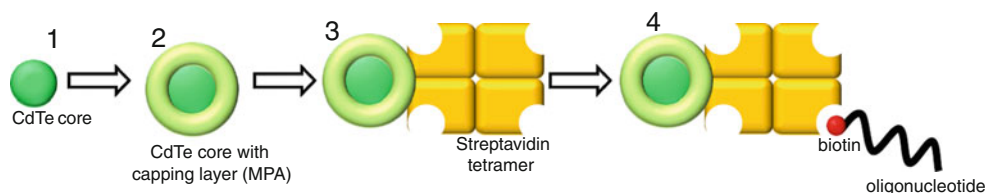


**Fig. 1** Scheme of the formation of the streptavidin-modified CdTe QDs. 1 metallic core of the CdTe QD; 2 capping with mercaptopropionic acid (MPA); 3 coupling with streptavidin; 4 interaction of streptavidin-modified QDs with biotinylated oligonucleotide



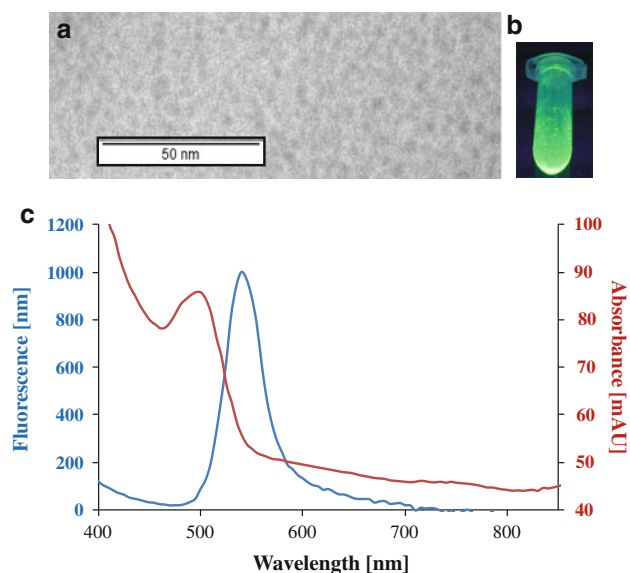


**Fig. 2** Characterization CdTe QDs. **a** TEM micrograph of the MPA capped CdTe QDs. **b** Photograph of the streptavidin-modified CdTe QDs under UV light illumination (260 nm). **c** Absorption and emission spectrum ( $\lambda_{\text{ex}} = 350 \text{ nm}$ )

After that we found that we synthesized nanoparticles of assumed composition, we aimed our attention at their fluorescent properties. The solution of CdTe QDs under UV light illumination (260 nm) is shown in Fig. 2b and the fluorescence and absorbance spectra of the prepared QDs are shown in Fig. 2c. It clearly follows from these results that the emission maximum of the streptavidin-modified CdTe QDs (QDs-MPA-strep) is at 550 nm and therefore strong green emission is observed. In the absorption

spectrum, except strong absorption in UV region, maximum at 495 nm was observed.

#### Electrophoretic Characterization of CdTe QDs

Streptavidin is a 60 kDa protein purified from the bacterium *Streptomyces avidinii* composed of four identical streptavidin monomer units with extraordinarily high affinity for biotin [42]. The analysis of streptavidin by SDS-PAGE confirmed that QDs-MPA-strep contained streptavidin in form of monomer, dimer and tetramer (Fig. 3a). To compare electrophoretic behavior, the streptavidin standard and QDs-MPA-strep conjugate were observed both under reducing (lanes 2 and 4) and non-reducing conditions (lane 3 and 5). Under non-reducing conditions main band corresponding to streptavidin tetramer (60 kDa) was observed both in streptavidin standard and QDs-MPA-strep. Except these two, bands corresponding monomeric (15 kDa) and dimeric form (25 kDa) were observed. Although same protein amount was loaded, the band at QDs-MPA-strep appears less intensive and higher portion of streptavidin monomer is present. Under reducing conditions at streptavidin standard two bands corresponding to monomeric and dimeric form were observed, but at QDs-MPA-strep only one band corresponding to monomer was present. The increase of monomeric form of streptavidin at QDs-MPA-strep conjugate observed both under reducing and non-reducing conditions might cause decomposition of tetrameric form of streptavidin as a consequence of QDs binding.

Gel electrophoresis is however unable to distinguish between streptavidin and QDs-MPA-strep probably due to the low separation power and expected small difference in

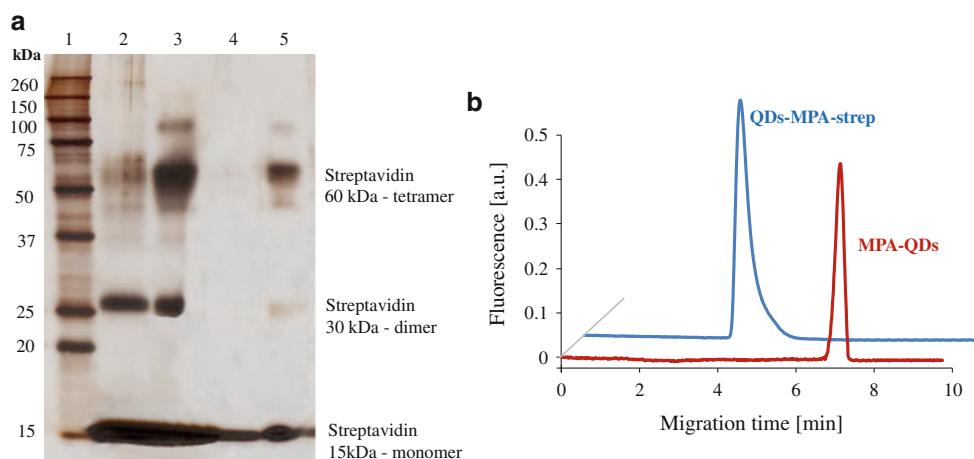


**Fig. 3** Electrophoretic characterization of the QDs solution. **a** SDS-PAGE of streptavidin and QDs-MPA-strep under reducing and non-reducing conditions, (acrylamide gel: 10 % (m/V) separation gel, 5 % (m/V) stacking gel, separation voltage: 150 V for 1 h at 23 °C, electrolyte: 0.025 M Trizma-base, 0.19 M glycine and 3.5 mM SDS, pH = 8.3). Silver staining according to Krizkova et al. [40],

1 Molecular weight standard, 2 Streptavidin Reducing, 3 Streptavidin Non-reducing, 4 QDs-MPA-strep Reducing, 5 QDs-MPA-strep Non-reducing; **b** CE-LIF analysis of QDs-MPA-strep and MPA-QDs (electrolyte: 0.02 M sodium borate, voltage: 20 kV, capillary: 47/40 cm, 75  $\mu\text{m}$  ID, injection : 20 s, 3.4 kPa)

molecular mass of streptavidin itself and QDs-MPA-strep. The migration behaviour of QDs-MPA in SDS-PAGE may be different from the proteins such as the molecular weight standards and streptavidin, therefore, it might be difficult to estimate the molecular mass of QDs-MPA by the SDS-PAGE. Moreover, CE-LIF was used to prove the bioconjugation of CdTe QDs. As shown above, the absorption maximum at 495 nm enabled the Ar<sup>+</sup> laser with emission wavelength of 488 nm to be used as an excitation light source. Electropherograms showed in Fig. 3b indicates that the migration time of MPA-QDs is 7.1 min; however, the peak of QDs-MPA-strep has the migration time of 4.2 min. The electrophoretic mobilities calculated for MPA-QDs and QDs-MPA-strep were  $-27.82 \times 10^{-9} \text{ m}^2/\text{V/s}$  and  $-9.87 \times 10^{-9} \text{ m}^2/\text{V/s}$ , respectively (calculated according to the Eq. 1).

$$\mu = \frac{L \times l}{V} \times \left( \frac{1}{t} - \frac{1}{t_0} \right) \quad (1)$$

where  $\mu$  is electrophoretic mobility,  $L$  is total capillary length,  $l$  is effective capillary length,  $V$  is applied voltage,

$t_0$  is migration time of EOF marker and  $t$  is analyte migration time.

Due to the selectivity of laser-induced fluorescence detection, which is enabling only fluorescent molecules to be detected and significant differences of electrophoretic mobilities of MPA-QDs and QDs-MPA-strep, it can be concluded that bioconjugation was successful.

#### CE-LIF of CdTe QDs Oligonucleotides

Even though the LIF detection provides excellent selectivity, the UV absorbance detection was used for further CE analyses offering the versatility needed for monitoring of the interactions in the solutions. This powerful combination of detection modalities enabled detail monitoring of complex formation and identification of reaction components. After verification of successful surface modification of CdTe QDs by streptavidin, the functionality was confirmed by interaction with biotinylated oligonucleotide. The first model oligonucleotide was the fragment of BCL-2 gene. CE-UV electropherograms of individual components

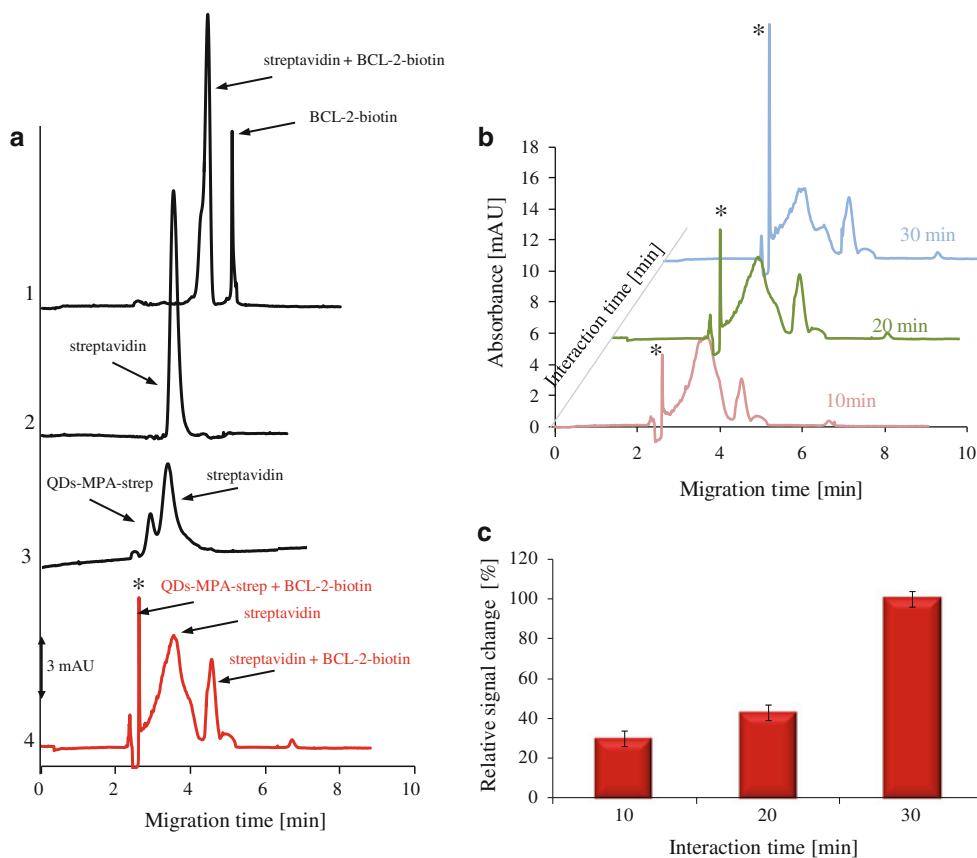


**Fig. 4** Monitoring of interaction of QDs-MPA-strep with biotinylated BCL-2 oligonucleotide. **a** CE-UV identification of mixture components, 1 mixture of streptavidin with biotinylated BCL-2 oligonucleotide, 2 streptavidin, 3 QDs-MPA-strep solution, mixture of QDs-MPA-strep solution with biotinylated BCL-2 oligonucleotide,

(asterisk) complex of QDs-MPA-strep and BCL-2-biotin (electrolyte: 0.02 M sodium borate, voltage: 20 kV, capillary: 47/40 cm, 75  $\mu\text{m}$  ID, injection : 20 s, 3.4 kPa). **b** Time dependence of the formation of QDs-MPA-strep-BCL-2-biotin complex. **c** Time dependent increase of the complex signal

of the reaction mixture are shown in Fig. 4a. It follows from the results that BCL-2 oligonucleotide gave a sharp peak with migration time of 5.19 min and electrophoretic mobility of  $-35.09 \times 10^{-9} \text{ m}^2/\text{V/s}$ . During the interaction with streptavidin, a peak of the complex with the migration time of 4.52 min and electrophoretic mobility of  $-30.70 \times 10^{-9} \text{ m}^2/\text{V/s}$  was formed. Streptavidin peak had the migration time of 3.42 min and electrophoretic mobility of  $-19.47 \times 10^{-9} \text{ m}^2/\text{V/s}$ . The electropherogram of QDs-MPA-strep gave two peaks corresponding to the streptavidin excess (electrophoretic mobility  $-19.47 \times 10^{-9} \text{ m}^2/\text{V/s}$ ) and QDs-MPA-strep with electrophoretic mobility of  $-10.02 \times 10^{-9} \text{ m}^2/\text{V/s}$ . Comparing the electrophoretic mobilities obtained for QDs-MPA-strep by CE-LIF and CE-UV, we found that they are in a good agreement enabling us to identify the peak of QDs-MPA-strep in the CE-UV electropherogram. Finally, the electropherogram of the mixture of biotinylated BCL-2 oligonucleotide and QDs-MPA-strep (red line) is shown in Fig. 4a (sample of oligonucleotide was mixed with quantum dots in 1:1 ratio (v/v) and the final concentration of oligonucleotide was  $5 \mu\text{M}$ ). A number of signals occurred in this electropherogram with migration times corresponding to streptavidin, streptavidin-BCL-2-biotin complex and a very sharp peak (marked with a star). This peak probably belongs to the complex of QDs-MPA-strep and oligonucleotide BCL-2-biotin. As shown in Fig. 4b and c, the signal intensity of this peak increased with time of

interaction between the QDs-MPA-strep and BCL-2-biotin solution.

The interaction of QDs-MPA-strep was verified also by second oligonucleotide fragment, specific for hepatitis B virus labelled with biotin (HBV-biotin). There was no aim to separate BCL-2 from HBV. The electropherogram of the mixture of QDs-MPA-strep and HBV-biotin oligonucleotide contained a peak of unreacted HBV-biotin oligonucleotide at migration time of 4.92 min, unreacted streptavidin at migration time of 3.49 min and a peak of the complex QDs-MPA-strep + HBV-biotin at migration time of 2.8 min (Fig. 5a). The signal intensity of this peak increased with time (Fig. 5b, c). During 30 min of interaction the intensity of this peak increased to 27 mAU in comparison to BCL-2-biotin oligonucleotide, where the increase in the signal was 15.5 mAU only.

### Gel Electrophoresis of CdTe QDs Oligonucleotides

After that we characterized the complex by CE, agarose gel electrophoretic was used to detect DNA (Fig. 6a). In the lane 2, MPA-QDs were injected exhibiting no signal, but in the lane 3 streptavidin-modified CdTe QDs coupled to biotinylated HBV oligonucleotide were injected showing a weak signal (marked by arrow) confirming the presence of oligonucleotide. In the lane 4, QDs-MPA-strep were injected and as expected no DNA-specific signal was observed. Lane 5 was filled by streptavidin and there was a

**Fig. 5** Monitoring of the interaction of QDs-MPA-strep with biotinylated HBV oligonucleotide. **a** CE-UV identification of mixture components 1 biotinylated HBV oligonucleotide, 2 streptavidin, 3 QDs-MPA-strep solution, mixture of QDs-MPA-strep solution with biotinylated HBV oligonucleotide, (asterisk) complex of QDs-MPA-strep and HBV-biotin (for other experimental conditions see caption for Fig. 4). **b** Time dependence of the formation of QDs-MPA-strep-HBV-biotin complex. **c** Time dependent increase of the complex signal

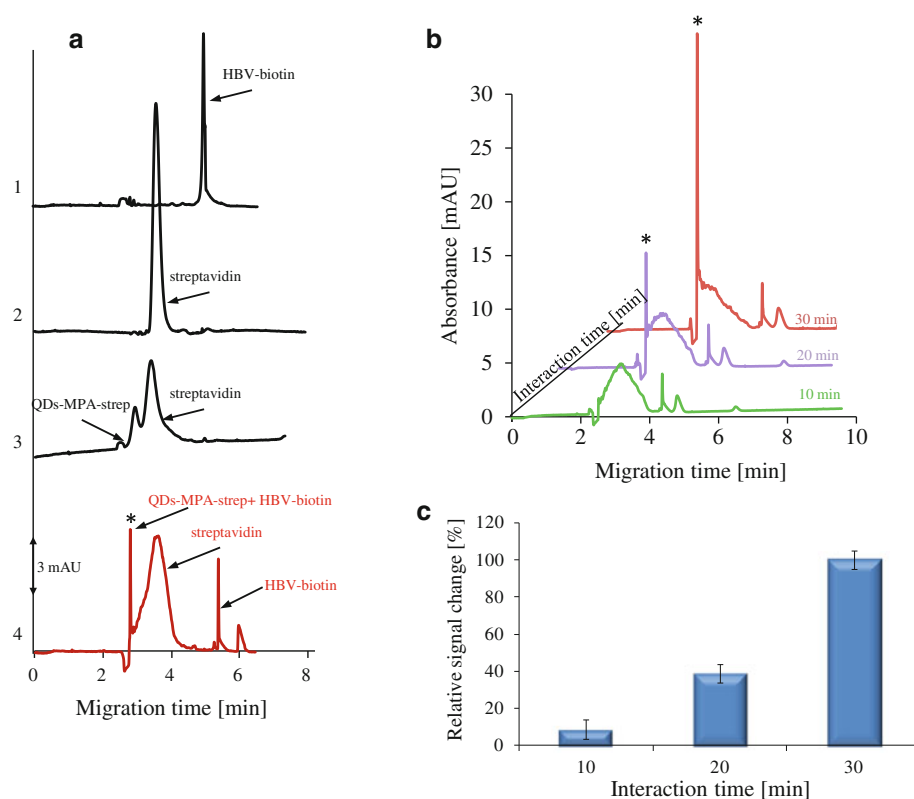
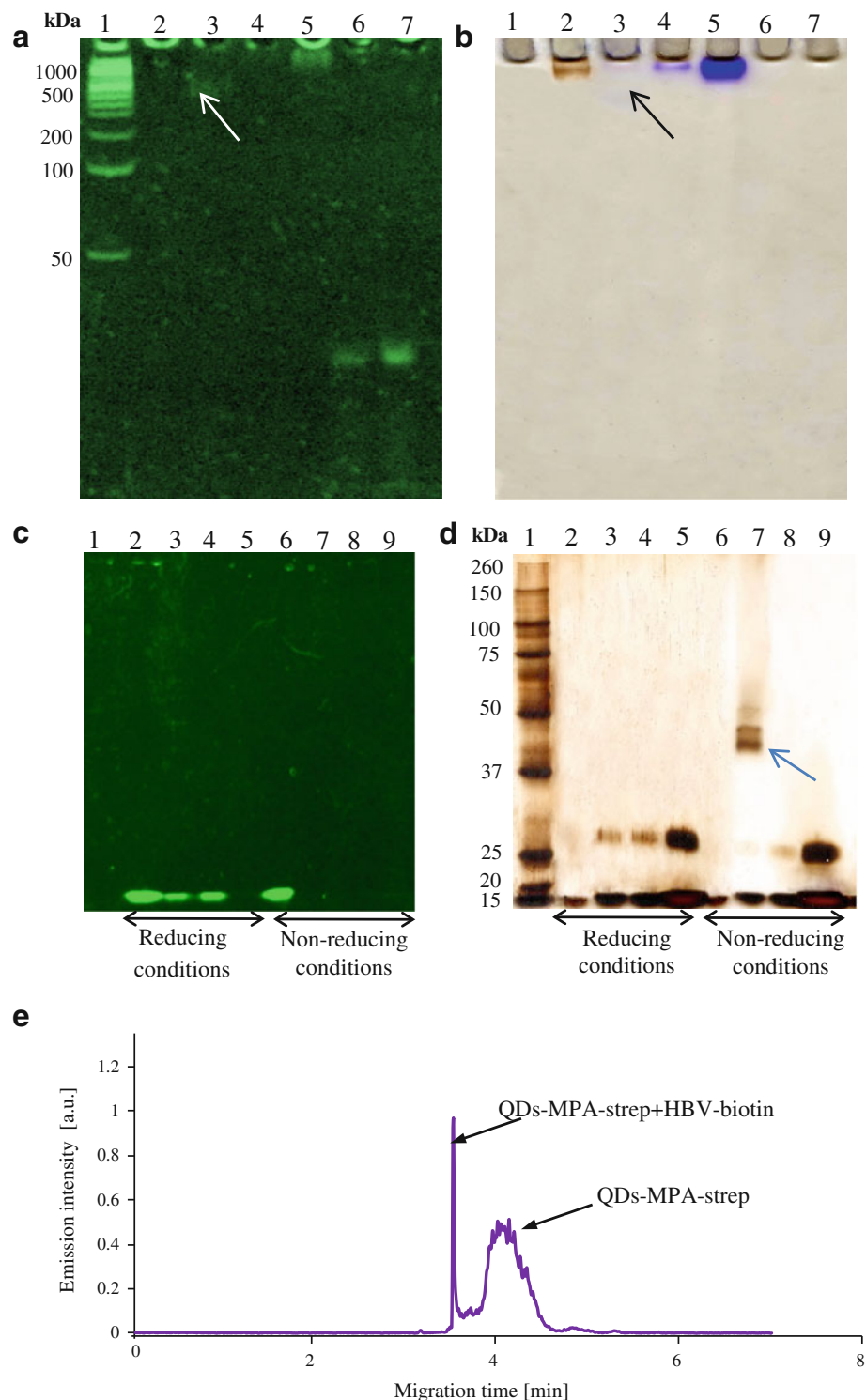




**Fig. 6** **a** Agarose gel electrophoresis labelled by DNA-specific staining (GelRed™) visualized by fluorescence under 510 nm illumination and emission at 600 nm, 1 Ladder, 2 MPA-QDs, 3 QD-MPA-strep-VHB-biotin, 4 QDs-MPA-strep, 5 Streptavidin, 6 BCL-2-biotin, 7 VHB-biotin. **b** Agarose gel electrophoresis labelled by protein-specific staining—Coomassie blue, lane captions same as in (b). **c** SDS-PAGE non-labelled, visualized by fluorescence under 470 nm illumination and emission at 535 nm, 1 Ladder, 2 MPA-QDs, 3 QD-MPA-strep-VHB-biotin, 4 QDs-MPA-strep, 5 Streptavidin, 6 MPA-QDs, 7 QD-MPA-strep-VHB-biotin, 8 QDs-MPA-strep, 9 Streptavidin (2–5 reducing conditions, 6–9 non-reducing conditions). **d** SDS-PAGE labelled by silver, lane captions same as in (c). **e** CE-LIF identification of complex of QDs-MPA-strep + biotinylated HBV oligonucleotide (electrolyte: 0.02 M sodium borate, voltage: 20 kV, capillary: 47/40 cm, 75 μm ID, injection : 20 s, 3.4 kPa)



remarkable signal visible, however we believe that it is an undesirable artefact, because DNA-specific staining should not be able to label this protein. In lanes 6 and 7, oligonucleotides BCL-2 and HBV were injected, respectively and bands can be seen in the low-molecular mass region.

In Fig. 6b, the same gel as in Fig. 6a was used; however, protein-specific staining by Coomassie blue was used. In

lanes 1, 6 and 7, no signal were observed due to the presence of DNA only. In the lane 2, a brown band was visible corresponding probably to the MPA-QDs damaged by precipitation in the staining solutions. In the lane 3, a very weak signal occurred under careful observation (marked by arrow). Based on the comparison to the signal in the Fig. 6a (in the same position), it can be concluded

that both DNA and proteins are present, however, in very low concentrations. This leads us to the opinion that this band corresponds to the complex of MPA-QD-strep with biotinylated HBV oligonucleotide. Lane 4 contained MPA-QD-strep, which was confirmed by band of streptavidin at the beginning of the lane. Similarly, in the lane 5, the intensive signal of streptavidin standard was detected. It should be noted that agarose gel electrophoresis is optimized for DNA separation and therefore, poor migration of analytes not containing DNA is observed. On the other hand, it clearly follows from the results obtained that the migration of the complex of MPA-QD-strep with biotinylated oligonucleotide was significantly improved due to the presence of DNA fragment.

To support our hypothesis, SDS-PAGE analysis was carried out under both reducing and non-reducing conditions. At first, the separated analytes were analysed with fluorescent visualization under illumination by light with 480-nm wavelength. Several intensive signals are present due to the intrinsic fluorescence of QDs (Fig. 6c). In lane 1, only the protein ladder was injected and therefore no fluorescence is observed, however in lanes 2, 3, and 4 samples containing MPA-QDs, QD-MPA-strep-VHB-biotin and QDs-MPA-strep were injected, respectively. Interestingly, all these samples maintained their fluorescent properties even though they did not differ in migration through the gel. In lane 5, streptavidin standard was injected and therefore no fluorescence was observed. Lanes 6–9 were analysed under non-reducing conditions, and fluorescent signal was observed only in the lane 6 injected with MPA-QDs. In lanes 7 and 8, the fluorescence of QDs was quenched by the conditions.

Subsequently, the gel was stained with silver to visualize the proteins (Fig. 6d). In lane 2, signal at molecular mass of 15 kDa was detected, however due to the absence of proteins it can be concluded that the signal belongs to the MPA-QDs. In lanes 3 and 4, two bands at molecular masses of 15 and 30 kDa occurred. The band at 15 kDa belongs to the MPA-QD-strep and the band at 30 kPa belongs to the streptavidin dimer due to the excess of the streptavidin in the solution. The signals in lanes 3 and 4 are very similar because the presence of the biotinylated oligonucleotide did not influence the migration under protein-specific conditions. Finally, streptavidin standard was injected in lane 5 confirming that monomer and dimer forms of this protein were in the solution used for modification of MPA-QDs. Under non-reducing conditions, significant changes are present. In lane 6, only a band of MPA-QDs with molecular mass of approx. 15 kDa was observed, however in lane 7, number of bands at molecular masses of 40–50 kDa were visible. As known from the literature [43], under non-reducing conditions the biotin bound to the streptavidin causes the streptavidin units not to be divided. This leads us

to the conclusion that the complex of MPA-QD-strep-HBV-biotin is formed and these bands belong to this complex. In contrary in lane 8, in which sample of MPA-QD-strep is injected only; no such shift was observed. Finally, the streptavidin standard injected in lane 9 provided signals of monomeric and dimeric forms only.

For final verification of MPA-QD-strep-HBV-biotin complex formation, CE–LIF was used taking advantage of the selectivity of fluorimetric detection neglecting non fluorescent components of the solution such as unreacted oligonucleotide as well as unreacted streptavidin. Two distinguished signals are present in the electropherogram, shown in Fig. 6e. The broad peak with migration time of approx. 4 min belongs to the QDs-MPA-strep and the sharp peak with migration time of 3.5 min belongs to the complex of MPA-QD-strep-HBV-biotin.

## Conclusion

It clearly follows from the obtained results that successful synthesis of MPA capped CdTe QDs was performed followed by functionalization by streptavidin enabling the bioconjugation with biotinylated analytes such as oligonucleotides. The quality of prepared MPA-QDs-strep as well as their interaction with selected oligonucleotides was verified by CE–UV and CE–LIF methods. By combination of gel electrophoresis and CE, the efficiency of functionalization process as well as monitoring of the interactions was verified. Importance of streptavidin–biotin linkage relies on numerous of biomolecules, which can be easily biotinylated and through it rather than linked with streptavidin. In this paper, this linkage was used as streptavidin-modified QDs to label and detect biotinylated oligonucleotide cancer sequence of BCL-2 and sequence of virus hepatitis B (VHB). This detection might help to have fast and precise diagnosis of these diseases in the future.

**Acknowledgments** Financial support from the following projects NanoBioTECell GA CR P102/11/1068, IGA IP10/2012 and CEITEC CZ.1.05/1.1.00/02.0068 is highly acknowledged.

## References

- Perez-Ruiz T, Martinez-Lozano C, Sanz A, Bravo E (2003) *Chromatographia* 58:757–762
- Tanaka Y, Terabe S (1999) *Chromatographia* 49:489–495
- Green NM (1990) *Method Enzymol* 184:51–67
- Sakahara H, Saga T (1999) *Adv Drug Deliv Rev* 37:89–101
- Caswell KK, Wilson JN, Bunz UHF, Murphy CJ (2003) *J Am Chem Soc* 125:13914–13915
- Roco MC, Mirkin CA, Hersam MC (2011) *J Nanopart Res* 13:897–919
- Chomoucka J, Drbohlavova J, Huska D, Adam V, Kizek R, Hubalek J (2010) *Pharmacol Res* 62:144–149

8. Prasek J, Drbohlavova J, Chomoucka J, Hubalek J, Jasek O, Adam V, Kizek R (2011) *J Mater Chem* 21:15872–15884
9. Drbohlavova J, Chomoucka J, Adam V, Ryvolova M, Eckschlager T, Hubalek J, Kizek R (2012) *Curr Drug Metab* (in press)
10. Chomoucka J, Drbohlavova J, Masarik M, Ryvolova M, Huska D, Prasek J, Horna A, Trnkova L, Provaznik I, Adam V, Hubalek J, Kizek R (2012) *Int J Nanotechnol* 9:746–783
11. Sahoo SK, Parveen S, Panda JJ (2007) *Nanomed Nanotechnol Biol Med* 3:20–31
12. Rao CNR, Kulkarni GU, Thomas PJ, Edwards PP (2002) *J Chem Eur* 8:29–35
13. Yu WW, Chang E, Drezek R, Colvin VL (2006) *Biochem Biophys Res Commun* 348:781–786
14. Bharali DJ, Mousa SA (2010) *Pharmacol Ther* 128:324–335
15. Mudshinge SR, Deore AB, Patil S, Bhalgat CM (2011) *Saudi Pharm J* 19:129–141
16. Walling MA, Novak JA, Shepard JRE (2009) *Int J Mol Sci* 10:441–491
17. Ryvolova M, Chomoucka J, Janu L, Drbohlavova J, Adam V, Hubalek J, Kizek R (2011) *Electrophoresis* 32:1619–1622
18. Trojan V, Chomoucka J, Krystofova O, Hubalek J, Babula P, Kizek R, Havel L (2010) *J Biotechnol* 150:S479–S479
19. Wang C, Gao X, Ma Q, Su XG (2009) *J Mater Chem* 19:7016–7022
20. Zheng YG, Gao SJ, Ying JY (2007) *Adv Mater* 19:376–380
21. Liu WH, Choi HS, Zimmer JP, Tanaka E, Frangioni JV, Bawendi M (2007) *J Am Chem Soc* 129:14530–14531
22. Huang XY, Weng JF, Sang FM, Song XT, Cao CX, Ren JC (2006) *J Chromatogr A* 1113:251–254
23. Aoyagi S, Kudo M (2005) *Biosens Bioelectron* 20:1680–1684
24. Xiao Y, Barker PE (2004) *Nucleic Acids Res* 32:e28
25. Smith AM, Duan HW, Mohs AM, Nie SM (2008) *Adv Drug Deliv Rev* 60:1226–1240
26. Wilcoxon JP, Martin JE, Provencio PP (2000) *Langmuir* 16:9912–9920
27. Kirkland JJ (1979) *J Chromatogr* 185:273–288
28. Kazakov S, Kaholek M, Kudasheva D, Teraoka I, Cowman MK, Levon K (2003) *Langmuir* 19:8086–8093
29. Li YQ, Wang HQ, Wang JH, Guan LY, Liu BF, Zhao YD, Chen H (2009) *Anal Chim Acta* 647:219–225
30. Vanifatova NG, Spivakov BY, Mattusch J, Franck U, Wennrich R (2005) *Talanta* 66:605–610
31. Alonso MCB, Prego R (2000) *Anal Chim Acta* 416:21–27
32. Liu FK, Tsai MH, Hsu YC, Chu TC (2006) *J Chromatogr A* 1133:340–346
33. Schnabel U, Fischer CH, Kenndler E (1997) *J Microcolumn Sep* 9:529–534
34. Krupke R, Hennrich F, von Lohneysen H, Kappes MM (2003) *Science* 301:344–347
35. Olivas WM, Maher LJ (1996) *Nucleic Acids Res* 24:1758–1764
36. Kondili L, Argentini C, La Sorsa V, Chionne P, Costantino A, Mele A, Brunetto MR, Rapicetta M (2002) *J Hepatol* 36:224–225
37. Duan JL, Song LX, Zhan JH (2009) *Nano Res* 2:61–68
38. Baumle M, Stamou D, Segura JM, Hovius R, Vogel H (2004) *Langmuir* 20:3828–3831
39. Wong C, Sridhara S, Bardwell JCA, Jakob U (2000) *Biotechniques* 28:426–428
40. Krizkova S, Adam V, Eckschlager T, Kizek R (2009) *Electrophoresis* 30:3726–3735
41. Algar WR, Tavares AJ, Krull UJ (2010) *Anal Chim Acta* 673:1–25
42. Petrlova J, Masarik M, Potesil D, Adam V, Trnkova L, Kizek R (2007) *Electroanalysis* 19:1177–1182
43. O'Sullivan VJ, Barrette-Ng I, Hommema E, Hermanson GT, Schofield M, Wu S-C, Honetschlaeger C, Ng KKS, Wong S-L (2012) *PLoS ONE* 7:e35203